Remote Sensing of Environment 115 (2011) 1955–1965

Contents lists available at ScienceDirect

Remote Sensing of Environment

journal homepage: www.elsevier.com/locate/rse

Comparison of three SeaWiFS atmospheric correction algorithms for turbid waters using AERONET-OC measurements

Cédric Jamet [a,b,*], Hubert Loisel [a,b], Christopher P. Kuchinke [c], Kevin Ruddick [d], Giuseppe Zibordi [e], Hui Feng [f]

[a] Univ Lille Nord de France, ULCO, LOG, F-62930 Wimereux, France
[b] CNRS, UMR 8187, F-62930 Wimereux, France
[c] Department of Physics, University of Miami, PO Box 248046, Coral Gables, FL 33124, USA
[d] Management Unit of the North Sea Mathematical Models (MUMM), Royal Belgian Institute for Natural Sciences (RBINS), 100 Gulledelle, B-1200 Brussels, Belgium
[e] Joint Research Centre, Institute for Environment and Sustainability, Global Environment Monitoring Unit, Ispra, 21020, Italy
[f] Ocean Process Analysis Laboratory, Institute for the Study of Earth, Oceans and Space, University of New Hampshire, Durham, NH 03824, USA

ARTICLE INFO

Article history:
Received 4 August 2010
Received in revised form 16 March 2011
Accepted 21 March 2011
Available online 14 April 2011

Keywords:
Ocean color
Atmospheric correction
Remote sensing
Validation
AERONET-Ocean Color

ABSTRACT

The use of satellites to monitor the color of the ocean requires effective removal of the atmospheric signal. This can be performed by extrapolating the aerosol optical properties in the visible from the near-infrared (NIR) spectral region assuming that the seawater is totally absorbant in this latter part of the spectrum. However, the non-negligible water-leaving radiance in the NIR which is characteristic of turbid waters may lead to an overestimate of the atmospheric radiance in the whole visible spectrum with increasing severity at shorter wavelengths. This may result in significant errors, if not complete failure, of various algorithms for the retrieval of chlorophyll-*a* concentration, inherent optical properties and biogeochemical parameters of surface waters.

This paper presents results of an inter-comparison study of three methods that compensate for NIR water-leaving radiances and that are based on very different hypothesis: 1) the standard SeaWiFS algorithm (Stumpf et al., 2003; Bailey et al., 2010) based on a bio-optical model and an iterative process; 2) the algorithm developed by Ruddick et al. (2000) based on the spatial homogeneity of the NIR ratios of the aerosol and water-leaving radiances; and 3) the algorithm of Kuchinke et al. (2009) based on a fully coupled atmosphere–ocean spectral optimization inversion. They are compared using normalized water-leaving radiance nL_w in the visible. The reference source for comparison is ground-based measurements from three AERONET-Ocean Color sites, one in the Adriatic Sea and two in the East Coast of USA.

Based on the matchup exercise, the best overall estimates of the nL_w are obtained with the latest SeaWiFS standard algorithm version with relative error varying from 14.97% to 35.27% for $\lambda = 490$ nm and $\lambda = 670$ nm respectively. The least accurate estimates are given by the algorithm of Ruddick, the relative errors being between 16.36% and 42.92% for $\lambda = 490$ nm and $\lambda = 412$ nm, respectively. The algorithm of Kuchinke appears to be the most accurate algorithm at 412 nm (30.02%), 510 (15.54%) and 670 nm (32.32%) using its default optimization and bio-optical model coefficient settings.

Similar conclusions are obtained for the aerosol optical properties (aerosol optical thickness $\tau(865)$ and the Ångström exponent, $\alpha(510, 865)$). Those parameters are retrieved more accurately with the SeaWiFS standard algorithm (relative error of 33% and 54.15% for $\tau(865)$ and $\alpha(510, 865)$).

A detailed analysis of the hypotheses of the methods is given for explaining the differences between the algorithms. The determination of the aerosol parameters is critical for the algorithm of Ruddick et al. (2000) while the bio-optical model is critical for the algorithm of Stumpf et al. (2003) utilized in the standard SeaWiFS atmospheric correction and both aerosol and bio-optical model for the coupled atmospheric–ocean algorithm of Kuchinke. The Kuchinke algorithm presents model aerosol-size distributions that differ from real aerosol-size distribution pertaining to the measurements. In conclusion, the results show that for the given atmospheric and oceanic conditions of this study, the SeaWiFS atmospheric correction algorithm is most appropriate for estimating the marine and aerosol parameters in the given turbid waters regions.

1. Introduction

Coastal waters are ecologically very important and also a major resource for human populations because they contribute to a large share of the world fisheries catch and support the rapidly growing

* Corresponding author at: Univ Lille Nord de France, ULCO, LOG, F-62930 Wimereux, France.
E-mail address: cedric.jamet@univ-littoral.fr (C. Jamet).

0034-4257/$ – see front matter © 2011 Elsevier Inc. All rights reserved.
doi:10.1016/j.rse.2011.03.018

aquaculture industry. These waters are generally identified as Case II waters (Morel & Prieur, 1977), as opposed to Case I waters, because their optical properties cannot be solely defined as a function of a single phytoplankton-related parameter (due to contributions from non-co-varying terrestrial constituents such as detritus and colored dissolved organic matter (CDOM) from bottom resuspension and terrestrial origin). Because of the complexity of Case II waters, since the late 1970s most of the quantitative applications of ocean color remote sensing focused on Case I waters and were mostly restricted to the determination of the abundance and distribution of phytoplankton chlorophyll-*a*.

Since the Coastal Zone Color Scanner (CZCS) proof-of-concept ocean color mission (operating from 1978 to 1986), spaceborne monitoring of chlorophyll-*a* concentration has become well established and maintained through several satellite sensors including the Sea-Viewing Wide Field-of-View Sensor (SeaWiFS) launched in August 1997, the Moderate Resolution Imaging Spectroradiometers (MODIS) onboard the Terra and Aqua platforms in 1999 and 2002, respectively, and the Medium Resolution Imaging Spectrometer (MERIS) in 2002. The focus of the present study is on SeaWiFS, which now offers more than 13 years of data, giving the unique opportunity to study the long-term variability of the seawater properties at global and regional scales. This sensor has 6 spectral bands in the visible centered at $\lambda = 412$, 443, 490, 510, 555, and 670 nm and two bands in the near-infrared centered at $\lambda = 765$ and 865 nm.

The use of satellites to monitor the color of the ocean requires effective removal of the contribution of the atmosphere (due to absorption by gasses and aerosols, and scattering by air molecules and aerosols) to the total signal measured by the remote sensor at the top of the atmosphere, L_{toa}: the so called "atmospheric correction" process. The methods for removing the contribution of the atmosphere to the total measured signal exploit the high absorption by seawater in the red and near-infrared spectral regions. In open seawater, i.e. where generally chlorophyll-*a* concentration and related pigments and co-varying materials (like detritus) determine the optical properties of the ocean, seawater can be considered to absorb all light in the NIR so that the signal observed by the satellite sensor in this spectral domain is assumed to be entirely due to the atmospheric path radiance (L_A) and sea surface reflectance. This is not always the case when considering turbid waters (generally coastal optically complex waters). In these waters phytoplankton pigment and detritus, as well as suspended sediment, contribute to NIR backscatter. The resulting NIR water-leaving radiances introduce two sources of error into the removal of the aerosol. First, the total aerosol reflectance is overestimated as some of the total radiance (L_{toa}) at both 765 and 865 nm comes from the seawater. Second, as the absorption and scattering properties of seawater change from 765 to 865 nm, the selection of the appropriate atmospheric model is affected, causing an error in the extrapolation of L_A to shorter wavelengths. As a result, L_A is overestimated at all bands with increasing values at shorter wavelengths, even possibly leading to negative water-leaving radiances in the blue bands in coastal waters (Siegel et al., 2000). This results in severe errors, if not complete failure, for various algorithms to retrieve chlorophyll-*a* concentration and inherent optical properties relying on the spectral values of the water-leaving radiance.

To solve this problem, several atmospheric correction algorithms have been developed to process SeaWiFS data when normalized water-leaving radiance nL_w is non-negligible at NIR wavelengths (Bailey et al., 2010; Gould et al., 1998; Hu et al., 2000; Kuchinke et al., 2009a; Land & Haigh, 1996; Lavender et al., 2005; Oo et al., 2008; Ruddick et al., 2000; Shanmugam & Ahn, 2007; Stumpf et al., 2003). The existing large number of coastal water algorithms requires their inter-comparison to assess their accuracy since they are often based on quite different physical assumptions. However, only a few studies have been made to evaluate several algorithms from *in-situ* measurements (Banzon et al., 2009 for instance). More recently, a comparison of the standard atmospheric correction algorithms of the SeaWiFS, MODIS, MERIS, OCTS/GLI and POLDER sensors for the clear and turbid ocean has been made by a working group of the International Ocean Color Coordinating Group (IOCCG, 2010). This kind of exercise is fundamental to understand and compare retrievals from different sensors using different algorithms.

In this paper, three SeaWiFS data processing algorithms currently available in the SeaWiFS Data Analysis System (SeaDAS, Fu et al., 1998; Baith et al., 2001) are compared: the SeaWiFS standard algorithm (Bailey et al., 2010; Stumpf et al., 2003) and those proposed by Ruddick et al. (2000) and by Kuchinke et al. (2009a). The first two algorithms are based on the standard atmospheric correction of Gordon and Wang (1994), from herein referred to as GW94, and have been compared by Ransibrahmanakul et al. (2005), showing that the SeaWiFS standard algorithm provided the best estimates of the normalized water-leaving radiances using *in-situ* data along the U.S. coasts. The Kuchinke et al. (2009a) algorithm is an extension of the atmospheric correction of Chomko and Gordon (1998) and has been compared with the standard algorithm in Kuchinke et al. (2009b). This paper presents the first outcome of the ICAC inter-comparison project by comparing algorithms with *in situ* measurements of normalized water-leaving radiance (nL_w) made in coastal waters through the AERONET-Ocean Color network (thereafter AERONET-OC) of autonomous radiometers (Zibordi et al., 2006b, 2009). This network constitutes a unique dataset for assessment of the accuracy of satellite products in different coastal waters.

The results presented in this paper are based on data obtained with new SeaWiFS reprocessing released by NASA in fall 2009 and called R2009. The SeaWiFS standard NIR ocean contribution correction algorithm developed by Stumpf et al. (2003) and its update version (Bailey et al., 2010) is hereafter named S03, the NIR ocean contribution correction method developed by Ruddick et al. (2000) is named R00 and the atmospheric correction of Kuchinke et al. (2009a) is named K09. In the following sections, a short description of the three algorithms is presented showing their assumptions together with the details of the *in situ* measurements used for comparisons and the match-up protocol. The last two sections present the comparison analysis and a discussion on the limitations of the three algorithms.

2. Algorithms

The standard NIR ocean contribution correction method S03 and R00 evaluated in this study are based on the atmospheric correction algorithm initially developed for Case I waters by GW94. These algorithms extend the GW94 approach to waters where the black pixel assumption no longer holds (Siegel et al., 2000). The third algorithm, K09, contains its own independent atmospheric correction algorithm.

The top-of-atmosphere radiative signal can be expressed as:

$$\rho_{cor}(\lambda) = \rho_a(\lambda) + \rho_{ra}(\lambda) + t(\lambda)\cdot\rho_w(\lambda) = \rho_A(\lambda) + t^*(\lambda)\cdot\rho_w(\lambda) \quad (1)$$

where $\rho_{cor}(\lambda)$ is the top-of-atmosphere signal corrected for gas absorption, Rayleigh scattering, whitecaps and glitter (Gordon, 1997), $\rho_A(\lambda)$ is the reflectance due to the aerosol scattering and the interaction between molecular and aerosol scattering reflectance, $t^*(\lambda)$ is the diffuse transmittance through the atmosphere and $\rho_w(\lambda)$, the water-leaving reflectance. The goal of the atmospheric correction process is to quantify $\rho_A(\lambda)$ to determine $\rho_w(\lambda)$. The latter can then be used to assess the optical and biogeochemical properties of the seawater. In the rest of the paper, we will focus on the radiance instead of the reflectance, defined as: $L(\lambda) = \frac{\rho(\lambda)\cdot F_0\cdot \cos\theta_0}{\pi}$.

2.1. GW94-based with iterative procedure

The S03 method is based on an iterative procedure which is used to avoid the over-correction of the atmospheric signal. The procedure is

based on the original SeaWiFS processing code using GW94 atmospheric model. The goal is to remove L_w(NIR) from L_{cor}(NIR) so that only the atmospheric component of L_{cor}(NIR) is input into GW94. The iteration used L_{cor}(NIR) as input into GW94 in order to solve for L_w(670). Then, L_w(670) is used through a bio-optical model to determine L_w(NIR). This model is used to determine the backscatter at 670 nm, and specifically considers inorganic particles. This solution requires compensation for absorption by chlorophyll-*a*, detrital pigments and colored dissolved organic matter (CDOM). These are propagated to the top of the atmosphere (TOA). This TOA L_w(NIR) is removed from L_{cor}(NIR) which is then input into GW94 computation.

2.2. GW94-based with spatial homogeneity of NIR ratios of ρ_w and ρ_A

The second algorithm chosen uses an alternative method for estimating the marine contribution in the NIR as proposed by Ruddick et al. (2000). This algorithm replaces the assumption that the water-leaving radiance is zero in the NIR by the assumptions of spatial homogeneity of the 765/865 nm ratios for aerosol and water-leaving reflectances over the subscene of interest. The ratio of ρ_A reflectances at 765 and 865 nm is named ε and is considered as a calibration parameter to be calculated for each sub-scene of interest. In addition, the ratio of ρ_w at 765 and 865 nm, named α, is also considered as a calibration parameter and is fixed to a value 1.72 for the SeaWiFS sensor (Ruddick et al., 2000, 2006). These assumptions are used to extend to turbid waters the GW94. Using the definition of α and ε, the equations defining $\rho_A(765)$ and $\rho_A(865)$ become:

$$\rho_A(765) = \varepsilon(765,865).\left[\frac{\alpha\cdot\rho_{cor}(865)-\rho_{cor}(765)}{\alpha-\varepsilon(765,865)}\right] \quad (2)$$

$$\rho_A(865) = \frac{\alpha\cdot\rho_{cor}(865)-\rho_{cor}(765)}{\alpha-\varepsilon(765,865)} \quad (3)$$

The atmospheric correction algorithm can be summarized thus:

(1) Enter the atmospheric correction routine (i.e. GW94) to produce a scatter plot of Rayleigh-corrected reflectances $\rho_{cor}(765)$ and $\rho_{cor}(785)$ for the region of study. Select the calibration parameter ε on the basis of this scatter plot as described later.
(2) Reenter the atmospheric correction routine with data for Rayleigh-corrected reflectances $\rho_{cor}(765)$ and $\rho_{cor}(785)$ and use Eqs. (2) and (3) to determine $\rho_A(765)$ and $\rho_A(765)$, taking account of non-zero water-leaving reflectances.
(3) Continue as for the standard GW94 algorithm.

2.3. Spectral optimization algorithm

The algorithm K09 is a turbid-water adaptation of Chomko et al. (2003), named thereafter SOA, with improved atmospheric correction and scope to regionally tune the bio-optical model. It uses absorbing 'Haze-C' aerosol models (Chomko & Gordon, 1998) and a bio-optical reflectance model (Garver & Siegel, 1997, Maritonera et al., 2002; herein referred to as GSM) to provide the top-of-atmosphere (TOA) reflectance. The parameters of both models are then determined by fitting the modeled TOA reflectance to that observed from space, using non-linear optimization. Thus, it differs from GW94 in that all parameters are obtained simultaneously using all SeaWiFS bands. This is necessary in absorbing atmospheres where one can only 'see' aerosol absorption at wavelengths where high multiple scattering that exists, namely, the blue region of the visible spectrum. Since the GW94 atmospheric correction only uses NIR bands for its model selection, it cannot discern coastal aerosol absorption if it exists.

The SOA accounts for non-zero NIR water leaving reflectance by first assuming ρ_w(NIR) = 0 to provide initial estimates of ρ_A, and t* at NIR and visible wavelengths, and ρ_w at visible wavelengths. The retrieved apparent optical properties from GSM are then used to determine ρ'_w(NIR). The estimate of $t^*\rho'_w$(NIR) is then subtracted from the total reflectance to form the corrected reflectance, i.e.,

$$[\rho_A(NIR) + \rho_w(NIR)]^{(\text{Corrected})} = \rho_t(NIR) - \rho_r(\mathbb{N}IR) - t*(NIR)\rho'_w(NIR) \quad (4)$$

and the updated $\rho_A(NIR) + \rho_w(NIR)$ is used to initiate a new optimization, i.e., improved estimates of atmospheric parameters and subsequent calculation of new water parameters. The procedure iterates until the magnitude of $\rho_w(865)$ (or its difference across consecutive Case 2 loops, namely delta $\rho_w(865)$) falls below 0.0001. Since all models are coupled, the selection of bio-optical coefficients in K09 will have some effect on its atmospheric correction. In this study we elect to use the SeaDAS-default GSM Case 1 water bio-optical coefficients as determined by Maritonera et al. (2002).

3. Data

3.1. Satellite data

The satellite Level-1A data from SeaWiFS, onboard the OrbView-2 spacecraft, were acquired from the OBPG ocean color website (Feldman & McClain, 2009). Only the LAC (local-area coverage data) and MLAC (merged LAC, which consolidates all available full-resolution from a single orbit) full-resolution (1 km at nadir) imagery were considered. The satellite scenes corresponding to field measurements have been processed with the SeaDAS software package (version 6.1), using the latest SeaWiFS calibration.

The outputs of the SeaDAS processing are the normalized water-leaving radiance $nL_w(\lambda)$ at center wavelengths of 412, 443, 490, 510, 555 and 667 nm, denoted as $nL_w(412)$, $nL_w(443)$, $nL_w(490)$, $nL_w(510)$, $nL_w(555)$, $nL_w(670)$, respectively, the aerosol optical thickness, at $\lambda = 865$ nm, $\tau(865)$ and the Ångström coefficient determined from $\tau(\lambda)$ at $\lambda = 510$ nm and $\lambda = 865$ nm, $\alpha(510, 865)$, named hereafter, $\alpha(510)$.

3.2. Ground-based measurements

To estimate the accuracy of the values of $nL_w(\lambda)$ obtained from the three atmospheric correction algorithms, the retrievals were compared to *in situ* measurements of the normalized water-leaving radiance (nL_w) from AERONET-OC (Zibordi et al., 2006b, 2009). Three coastal stations were considered: the MVCO and COVE sites off the East Coast of the USA and the Acqua Alta Oceanographic Tower (AAOT) in the northern Adriatic Sea identified as Venise in the AERONET-OC database. Evaluations of the MODIS atmospheric and water products for the MVCO station have been published by Feng et al. (2008). Similar comparisons for the SeaWiFS, MERIS and MODIS products have been made for the AAOT and COVE sites (Melin et al., 2007; Zibordi et al., 2006a, 2009). The mean values and the standard deviations of these dataset are given in Table 1. The atmospheric and marine features of the three AERONET-OC sites have been extensively studied in the paper of Zibordi et al. (2009).

The AAOT site (Zibordi et al., 2006b) is located at 45.31°N; 12.50°E, 14.8 km off the Venice Lagoon in a frontal region that can be characterized by either Case I or Case II waters (Berthon & Zibordi, 2004). The Case II waters as classified by Loisel and Morel (1998), which represent a third of the measurement conditions, are mostly determined by the effects of river discharge and local winds. The aerosol type is mostly continental as influenced by atmospheric inputs from the nearby Po Valley. The dataset covers measurements over 68 months in the period from April 2002 to November 2007.

The MVCO site (Feng et al., 2008) is located at 41.33°N; 70.57°W, 3 km from the coast. As in the case of AAOT, there are spatial gradients in nL_w explained by a large variability in the seawater bio-optical properties. The seawater shows presence of highly absorbing dissolved

Table 1
Mean values and the standard deviation of *in-situ* $nL_w(\lambda)$, $\tau(865)$ and $\alpha(510)$ for the MVCO, AAOT and COVE stations.

		$nL_w(412)$	$nL_w(443)$	$nL_w(490)$	$nL_w(510)$	$nL_w(555)$	$nL_w(670)$	$\tau(865)$	$\alpha(510)$
MVCO	$\bar{x}\pm\sigma(x)$	0.45 ± 0.11	0.63 ± 0.19	0.99 ± 0.31	1.11 ± 0.35	1.18 ± 0.38	0.27 ± 0.11	0.054 ± 0.062	1.49 ± 0.46
AAOT	$\bar{x}\pm\sigma(x)$	0.92 ± 0.30	1.19 ± 0.43	1.64 ± 0.60	1.73 ± 0.60	1.60 ± 0.48	0.29 ± 0.11	0.080 ± 0.060	1.52 ± 0.51
COVE	$\bar{x}\pm\sigma(x)$	0.61 ± 0.27	0.88 ± 0.31	1.23 ± 0.40	1.35 ± 0.42	1.45 ± 0.42	0.39 ± 0.14	0.045 ± 0.040	1.09 ± 0.62
Global	$\bar{x}\pm\sigma(x)$	0.85 ± 0.32	1.10 ± 0.44	1.53 ± 0.59	1.62 ± 0.59	1.55 ± 0.48	0.29 ± 0.11	0.070 ± 0.054	1.48 ± 0.55

organic matter (Feng et al., 2008). In addition, this coastline is downwind of the North American continent, giving rise to an optically complex atmosphere. The aerosol distributions are highly variable in space and time with intermittent non-maritime aerosol (Hess et al., 1998). The dataset covers measurements over 14 months in the period from February 2004 to November 2005.

The COVE station is located on the Chesapeake Lighthouse platform 25 km from Virginia Beach, Virginia, near a transition region (36.9°N and 75.71°W) exhibiting large variability in the seawater bio-optical properties. The spectral features of nL_w are very similar to those detected at MVCO and suggest the presence of moderate concentration of sediments in the seawater (Zibordi et al., 2009). The dataset covers measurements over 24 months in the period from April 2006 to December 2008.

In situ AERONET-OC radiometric data at the MVCO, AAOT and COVE sites were collected in seven spectral bands centered at 412, 443, 531, 551, 667, 870 and 1020 nm (slightly different wavelengths were used during the testing phase of AERONET-OC).

4. Match-up protocol

4.1. Match-up construction

For the matchup exercise, a similar approach to that Bailey and Wang (2001) and Feng et al. (2008) has been used. First, a 2-hour time window is applied to the satellite overpass time at the measurement site to select satellite imagery. Second, the match-up procedure extracts a 2-by-3 pixel satellite image box with the northerly middle pixel closest to the measurement site when considering MVCO site. This configuration limits the effect of land on the match-up satellite data because MVCO site lies only 3 km south of the Martha's Vineyard coast. When considering the AAOT and COVE sites, a 3-by-3 pixel box is considered (centered on the middle pixel). Then, a valid pixel criterion is applied where a pixel is regarded as 'valid' if there exists none of the standard SeaWiFS Level-2 exclusion flags that include land mask, high sun glint, high solar zenith (higher than 70°), high satellite viewing zenith (higher than 60°), cloud or ice, and total radiance saturation. Furthermore, a match-up is accepted only if all 6 (9 for AAOT and COVE) pixels in the 2-by-3 (3-by-3 for AAOT and COVE) box are 'valid'. The mean value of $nL_w(\lambda)$ over the box under the defined criterion is calculated for each image. To choose the *in situ* data in the 2-hour interval, the measurement with the smallest time difference with each satellite measurement is selected. Lastly, an atmospheric spatial uniformity criterion is applied. This is based on a prescribed coefficient of spatial variation, defined as the ratio of the standard deviation to the mean pixel value within the selected image box. A match-up pair is accepted if the coefficient of spatial variation is <0.2 in $\tau(865)$.

4.2. Spectral match-up

The spectral channels of the SeaWiFS and AERONET-OC sensors differ slightly. These spectral differences were minimized through spline interpolation to adjust the AERONET-OC sensor channels to match the SeaWiFS channels. To validate the SeaWiFS Ångström exponent $\alpha(510, 865)$, a similar spline interpolation of the AERONET-OC aerosol optical thickness $\tau(\lambda)$ was applied to calculate the *in situ* $\tau(510)$. Then the *in situ* Ångström coefficient $\alpha(510, 865)$ was derived by using logarithm-transformed *in situ* $\tau(510)$ and $\tau(865)$.

5. Match-up results

In the following subsections, the statistical results are presented in terms of: root-mean-square-error (RMS), which gives the absolute scattering of the retrieved data:

$$RMS = \sqrt{\left(\sum\left(\frac{x^{mea}-x^{est}}{x^{mea}}\right)^2\right)\Big/ n}$$

the relative error expressed in percent, which represents the uncertainty associated with the satellite derived distribution:

$$relative\_error = \frac{1}{n}*\sum\left(\sqrt{\left(\frac{x^{mea}-x^{est}}{x^{mea}}\right)^2}\right)$$

the slope and intercept of the linear regression between the *in situ* and satellite values of the $nL_w(\lambda)$, $\tau(865)$ and $\alpha(510)$; and the correlation coefficient *r*. x^{mea} and x^{est} are the *in situ* and the SeaWiFS estimated measurements, respectively. We considered that all the errors are attributed to the satellite sensor and that the *in situ* data are considered as the "truth". Uncertainties for the AERONET-OC *in-situ* nL_w data are estimated less than 5% in the 412–551 nm spectral range and of approximately 8% at 667 nm (Zibordi et al., 2009).

Considering the criteria described in the previous sections and that only turbid waters, as defined by Robinson et al. (2003), are considered, 201 matchups were obtained for S03, 165 for R00, and 160 matchups for K09. The number of matchups for each site is given in Table 2 as well the number of negative values of $nL_w(412)$. S03 yields the greatest number of match-ups. This might indicate that this method provides a better spatial coverage of the marine and aerosol parameters or that the estimates from S03 are more homogeneous and less noisy. In this study, the negative values of $nL_w(412)$ in the blue band have been taken into account in the calculation of the statistics. There are 7 negative values for S03, 6 negative values for R00 and none for K09. The statistical results are given in Tables 3 and 5.

5.1. The marine parameters

As shown by Fig. 1, by regression lines and additionally in Table 3, all algorithms underestimate the values of nL_w at all wavelengths. This underestimation is less pronounced for S03. The best overall retrievals, i.e. with the lower error, are obtained with this latter algorithm with relative error varying from 14.97% at $\lambda = 490$ nm to 35.27% at $\lambda = 670$ nm. The method giving the least accurate normalized water-

Table 2
Number of matchups for each site and each algorithm.

	MVCO	AAOT	COVE	TOTAL	$nL_w(412)<0$
S03	20	163	18	201	7
R00	19	129	17	165	6
K09	13	134	13	160	0

Table 3
Statistical results for the retrieved values of $nL_w(\lambda)$ obtained with S03, R00 and K09.

	RMS	Relative error (%)	R	Slope	Intercept
$nL_w(412)$					
S03	0.322	31.36	*0.72*	*1.02*	*−0.08*
R00	0.360	36.81	0.68	0.85	−0.08
K09	*0.303*	*30.02*	0.68	0.86	0.004
nLw(443)					
S03	*0.318*	*21.81*	0.81	*1.00*	*−0.02*
R00	0.328	23.35	0.79	0.89	−0.02
K09	0.322	24.81	*0.85*	0.76	0.01
nLw(490)					
S03	*0.331*	*14.97*	*0.87*	*0.94*	*0.02*
R00	0.360	16.36	0.85	0.86	0.04
K09	0.412	20.53	0.85	1.07	0.08
nLw(510)					
S03	0.357	15.13	*0.85*	*0.90*	*0.03*
R00	0.393	17.15	0.83	0.81	0.09
K09	*0.340*	*14.54*	0.82	0.89	0.14
nLw(555)					
S03	*0.355*	*15.24*	*0.80*	*0.93*	*0.01*
R00	0.381	17.39	0.75	0.81	0.11
K09	0.388	17.64	0.73	0.94	0.07
nLw(670)					
S03	0.129	35.27	0.68	0.85	−0.03
R00	0.149	42.92	0.60	0.58	0.01
K09	*0.121*	*32.32*	*0.68*	0.61	0.03

The numbers in italic represent the best statistical results.

leaving radiances is R00, the relative error being between 16.36% at $\lambda = 443$ nm and 42.92% at $\lambda = 670$ nm. K09 shows the best retrievals at 412, 510 and 670 nm (RMS = 0.303 and relative error = 30.02% at 412 nm, for instance) while S03 is better at $\lambda = 443$, 490, 555 nm. However, none of the methods satisfies the requirements on the estimation of the nL_w (Hooker et al., 1992; IOCCG, 2000), i.e. RMS ~ 0.12 for $nL_w(443)$.

The RMS can also vary as a function of the wavelength (Fig. 2). The advantage of S03 is that the RMS is quite constant whatever visible wavelength is considered and thus the most stable of the three algorithms in the comparison. Even though K09 gives the best RMS and relative error for three wavelengths, those values seem to be wavelength-dependent as the RMS vary by a factor of 1.4 between its maximum (at $\lambda = 490$ nm) and minimum value (at $\lambda = 443$ nm).

To develop bio-optical algorithms, band ratios of the water-leaving radiances are often used (O'Reilly et al., 1998). Fig. 3 presents the comparison of the ratios $nL_w(443)/nL_w(555)$, $nL_w(490)/nL_w(555)$, and $nL_w(510)/nL_w(555)$ obtained with the three methods. Since the spectral relative error is constant for the S03, it is of no surprise that it retrieves the three ratios with the lowest errors. In contrast, the K09 is inconsistent across the three ratios as $nL_w(490)/nL_w(555)$ is highly overestimated. This is an artifact of the higher errors and RMS at 490 and 555 nm (see Table 3). The algorithm R00 is the least accurate. These results imply the relative effectiveness of each algorithm for use with empirical band-ratio bio-optical models. However, their drawback is that a 'good' ratio could be comprised of two equally bad wavelength comparisons (see Table 4).

5.2. The atmospheric parameters

In addition, we present the comparison of the aerosol parameters here. Though the focus of this paper is on the $nL_w(\lambda)$, it is interesting, also, to look at the aerosol optical parameters as it is often done. K09 does not retrieve directly the Angström exponent, α but it can be obtained through the SeaDAS software.

For the aerosol optical thickness $\tau(865)$ (Fig. 4, left panel), the SeaWiFS standard algorithm S03, is the most accurate algorithm and provides the best overall estimates with an RMS of 0.033 and a relative error of 33% (Table 5). The least accurate algorithm is K09 with an RMS of 0.041 and a relative error of 52.25%. S03 is very accurate for the low values of $\tau(865)$, but highly under-estimates the high values. K09 retrieves the high values ($\tau(865) > 0.2$) with an error of 17.7% and gives retrievals that are not biased as shown by the slope (0.99) and intercept (0.02) of the linear regression. The retrievals obtained with S03 and R00 are very similar and exhibit close values of RMS and relative errors.

From the aerosol optical thickness spectral values, the Ångström coefficient $\alpha(510, 865)$ can be calculated and estimated, which gives the spectral dependence of τ and is a proxy of the aerosol size. None of the algorithms is able to estimate the Ångström coefficient $\alpha(510, 865)$ (Fig. 4, right panel) with a high accuracy. The retrievals are relatively flat and patchy around the 1:1 line. The best method is S03 with an RMS of 0.566 and a relative error of 54.15% and the least accurate one is R00 (RMS of 0.618 and relative error of 71.15%).

6. Discussion

6.1. Analysis of the retrievals errors as function of environmental factors

To understand the capabilities of each method to deal with environmental parameters that can affect the accuracy of retrievals of $nL_w(\lambda)$, a study of the variation of the RMS and relative errors of $nL_w(\lambda)$ obtained with the three algorithms has been established as function of the turbidity, i.e. values of AERONET-OC $nL_w(670)$, the aerosol optical thickness at 865 nm, i.e. AERONET-OC $\tau(865)$ and the level of spatial homogeneity, i.e. $\frac{\sigma(\tau(865))}{\overline{\tau(865)}}$, where $\sigma(\tau(865))$ and $\overline{\tau(865)}$ are the standard deviation and mean of $\tau(865)$, respectively.

No clear trends were found from the inspection of the histograms (Fig. 5); no relations could be identified between these environmental factors and the retrieval errors for $nL_w(\lambda)$. S03 is the algorithm which provides most of the time, the best results whatever factor is considered. None of the algorithms have errors correlated to either the turbidity, or to the aerosol optical thickness or to the spatial heterogeneity.

The S03 algorithm is the least sensitive to the environmental factors as it provides the most overall accurate $nL_w(\lambda)$ for whatever value of the parameters is taken into account. However, K09 can be more accurate for specific ranges of those factors, especially for high values of the spatial homogeneity factor (Fig. 5). The R00 algorithm is the most sensitive method to the environmental factors than the two other algorithms.

6.2. Impact on the choice and estimation of the aerosol model

In order to understand the differences between the methods, it is necessary to understand the impact of the different aerosol models selected by each algorithm and the way to select the aerosol model for each pixel has to be understood. S03 and R00 differently address non-negligible NIR nL_w, even if though they are both based on the GW94 atmospheric correction scheme. They both partially couple the ocean and the atmosphere while K09 couples them totally.

Ahmad et al. (2010) state that the retrieved normalized water-leaving radiances values from the new set of aerosol models in S03 (and GW94) were essentially the same due to the approach employed for vicariously calibrating the water-leaving radiance retrievals, and because the new and old models can produce very similar spectral dependence. S03 and R00 take the same aerosol models but the hypotheses utilized for the selection of the aerosol models are quite different. Both base the selection of the aerosol model on the best-fit of an aerosol parameter, ε, which represents the 765/865 nm ratio of the aerosol reflectance. But in R00, this parameter is considered spatially homogeneous over the subscene of interest and has to be determined for each image. So the best-fit aerosol model will tend to

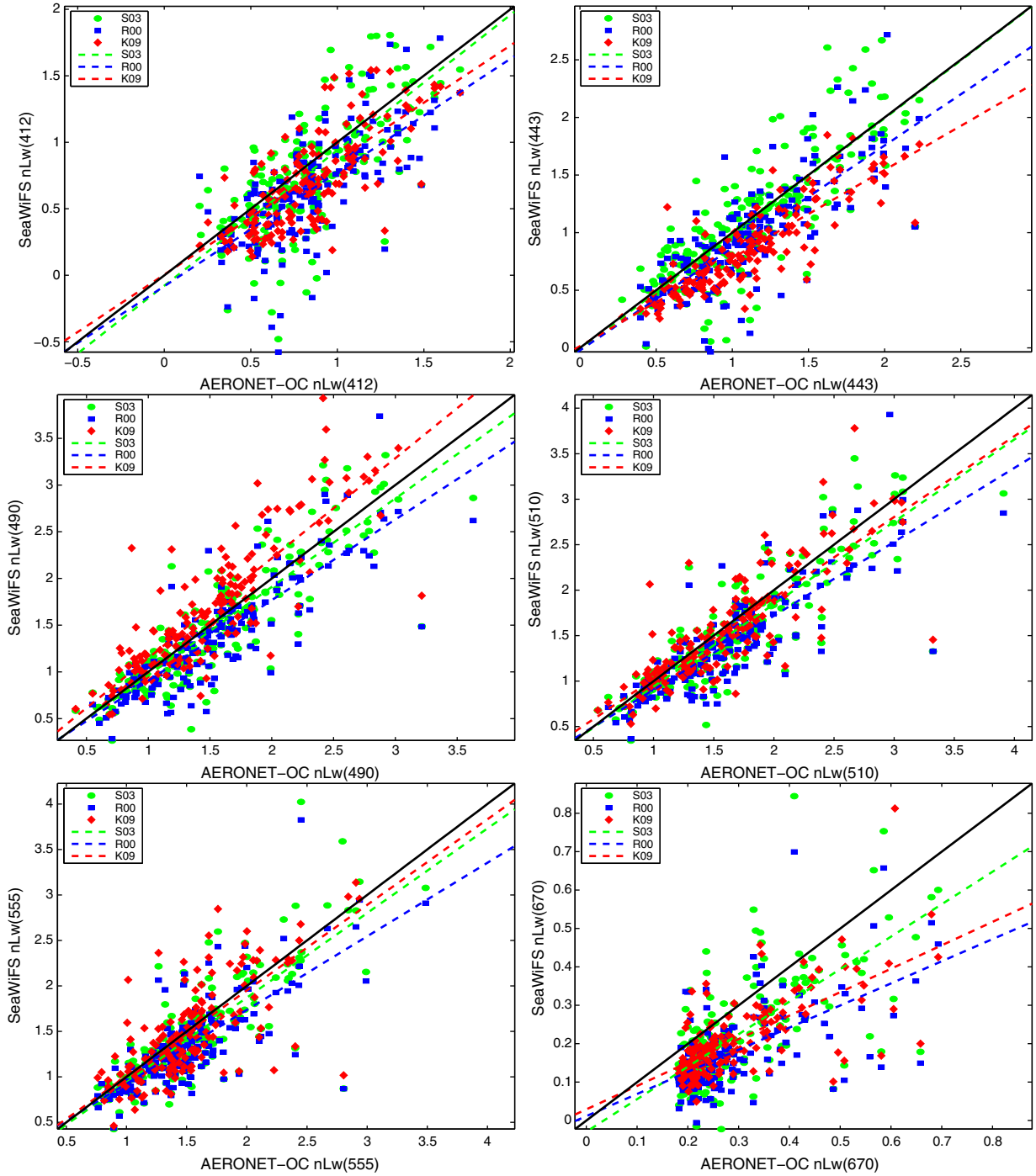

Fig. 1. Scatter plots of the retrieved $nL_w(\lambda)$ by S03(○), R00 (□) and K09 (◊) vs AERONET-OC measurements at the MVCO and AAOT sites. The black line represents the 1:1 line, the colored lines represent the linear regression lines for each algorithm.

be almost spatially homogeneous, with ε defined in GW94 almost equal to the calibration parameter defined by R00 and strictly equal on the single-scattering limit (Ruddick et al., 2000) To estimate this parameter, R00 uses the low Rayleigh-corrected L_{cor} corresponding to fairly clear waters where L_{cor} is considered to be dominated by aerosol reflectance. The threshold on the low Rayleigh-corrected L_{cor} is fixed in this study at 0.015. The aerosol parameter ε is calculated over the region of interest in the R00 (mean value) while it is calculated for each pixel in the S03 (a specific value for each pixel).

A sensitivity study on the impact of the values of ε(765, 865), as defined by R00 was performed by adding or sub-substracting a bias of 5, 10, 20 and 50%. We present here results when taking a positive bias of 10% that has been added to the original calculated value of ε(765, 865). Results clearly indicate that the value of ε(765, 865) plays a major role in the estimation of the oceanic and aerosol parameters. A positive bias to ε(765, 865) decreases the values of $nL_w(\lambda)$ and increases the values of α(510, 865) and τ(865). The effect of a different value of ε(765, 865) is more discernable on $nL_w(412)$, $nL_w(443)$, $nL_w(670)$ and α(510). When comparing the retrievals obtained with the positive 10% bias on ε(765, 865) to *in situ* measurements, the statistical results are somewhat similar, except for the correlation coefficients, slopes and intercepts of the regression lines. For instance,

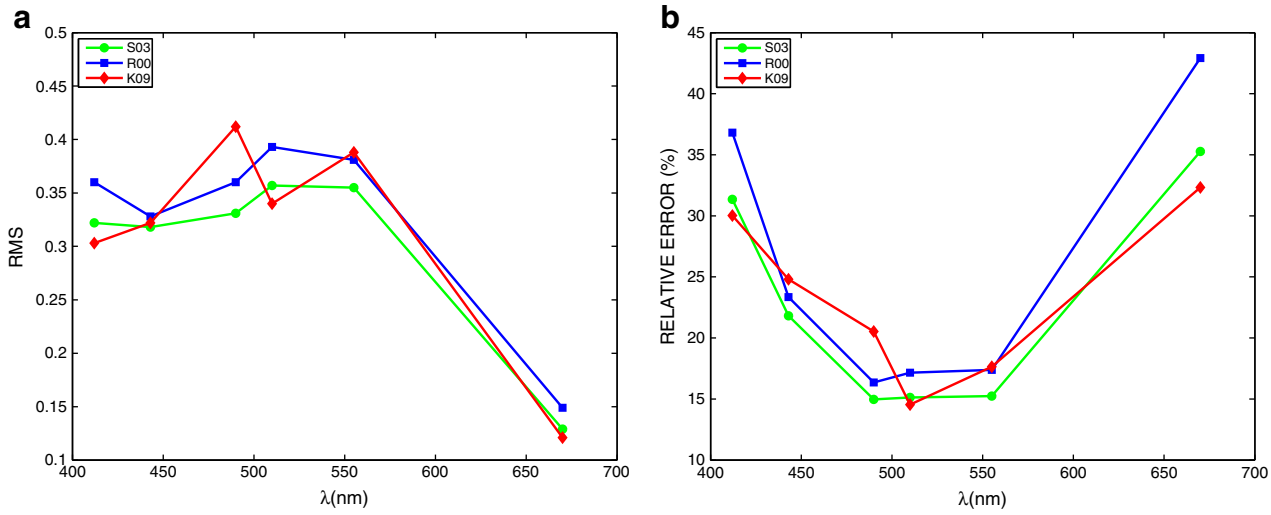

Fig. 2. Variation of the RMS (a) and the relative error (b) as a function of the wavelength.

for $nL_w(443)$, r increases from 0.79 to 0.88, the slope increases from 0.89 to 0.95. This means that the retrievals obtained with the bias on $\varepsilon(765, 865)$ are less biased than those obtained with its initial value. This trend is observed also for the aerosol optical thickness and for $\alpha(510, 865)$. So even with a small bias on the value of $\varepsilon(765, 865)$, the differences between the two ways of estimating nL_w are not negligible and it can be assumed that these differences will increase if the bias on $\varepsilon(765, 865)$ increases.

It is also observed that R00 is not symmetric with respect to positive/negative relative errors on $\varepsilon(765, 865)$. In particular, if $\varepsilon(765, 865)$ is overestimated, then more pixels will use the default GW94 method with zero $nL_w(NIR)$. However, if $\varepsilon(765, 865)$ is underestimated, the turbid water assumption will be applied to many more pixels. The sensitivity of R00 to $\varepsilon(765, 865)$ is considered a major problem for this algorithm. As this threshold on the low Rayleigh-corrected L_{cor} is determined empirically, those values may not be fully dominated by the aerosols and the threshold highly influences the retrievals. This is a drawback of the method and may explain the less accurate values of $nL_w(\lambda)$.

The aerosol models used in K09 are very different from those used in the SeaWiFS standard algorithm and in R00. As explained in Section 2.3, the aerosol models used in K09 have a Junge power-law size-distribution. The advantage of taking those models is that they are very well-suited for the optimization method (only the parameter, ν, is required to describe the aerosol size distribution, compared to several size distribution parameters in GW94). In offshore Case I waters the SOA has been shown to provide good accuracy in retrievals of apparent optical properties and hence La (Chomko et al., 2003). So far, results in some Case II waters are also satisfactory using K09 and references given earlier. This implies that for these studies, L_a was retrieved to reasonable accuracy (within 5%). This does not mean that the size distribution (or phase function) of K09 and GW94 will agree for similar nL_w (and hence L_a) matchups. An aerosol model that yields a phase function that approximates the true phase function is required to retrieve accurate aerosol optical values, even for weakly absorbing aerosols. But, this is not the case if the goal is to retrieve only L_a (see Gordon (1997) and Chomko and Gordon (1998)). This factor is likely to be important in this study where the real size distribution is likely to be biased towards one or several models, in this case possibly GW94. In this situation, K09 could give reasonable nL_w but unreasonable τ for example.

6.3. Hypothesis on the bio-optical models

The improvements in the NIR bio-optical model made by Bailey et al. (2010) in S03 allow to decrease the number of negative normalized water-leaving radiances in the blue (412 nm) by nearly half. The observed decrease in our study is 54% with our dataset (13 to 7 negative values).

The calibration parameter of the water-leaving reflectance ratio α in R00 has been set to a default value of 1.72. This ratio is used to evaluate the aerosol reflectance ρ_A (Eqs. 2, 3) in the NIR and its value can only be considered constant for weakly and moderately turbid waters while it varies for very turbid waters (Doron, 2007; Ruddick et al., 2006). Then if the value of the parameter is not exactly equal to 1.72, the incorrect estimation of the NIR ρ_A will occur, impact the proper choice of the aerosol model and thus lead to incorrect determination of the values of the water-leaving radiances in the visible channels.

The bio-optical algorithm utilized in K09, differs quite notably from the bio-optical model applied in the S03 and K00 (see Section 2.3). Because of the full spectrum coupled atmosphere–ocean approach of K09, it is difficult to quantify its performance for each individual scenario. In fact, even if $nL_w(\lambda)$ is error free, uncertainties in the coefficients of the bio-optical model may be the source of relative errors in the retrieved bio-optical parameters (Kuchinke et al., 2009a). Because it is a coupled model, error in one bio-optical coefficient may actually influence retrieval of all parameters, including those relating to the atmosphere. This is particularly true if the concentration of the bio-optical parameter which the coefficient is related to is high (e.g., colored detrital material). But one advantage of this method is that no negative nL_w are found in the short wavelengths. This is due to a constraint on $nL_w > 0$ applied during the optimization process.

6.4. Processing time

A comparison of the time-efficiency of the three algorithms is necessary for operational uses. S03 couples the advantage of being the best overall algorithm as well as being the most time-efficient. K09 is very time-consuming as is typical of any optimization method. For this algorithm, smaller images were processed (0.5°-by-0.5° instead of 4°-by-4° for S03 and R00). This is a main drawback of this algorithm. R00 is also quite efficient but less so than S03, as this method is a 2-step algorithm within the SeaDAS software. The first step is the calculation of the calibration parameter ε and the second step is used to perform the atmospheric correction. For series of images this first step will add time to the processing.

7. Conclusion

In this study, a comparison is made for SeaWiFS of two algorithms extending the "NIR black pixel" GW94 atmospheric correction

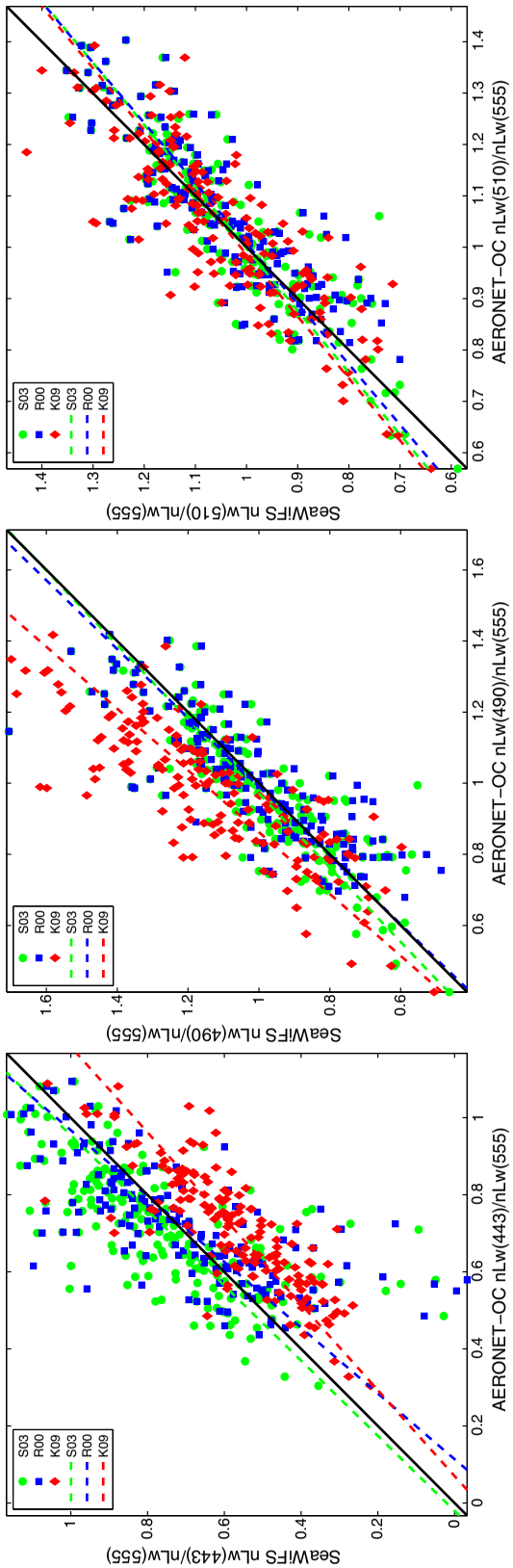

Fig. 3. Same as Fig. 1 but for the ratios from the left to the right: $nL_w(443)/nL_w(555)$, $nL_w(490)/nL_w(555)$, $nL_w(510)/nL_w(555)$.

Table 4
Statistical results for the retrieved values of three band ratios obtained with S03, R00 and K09.

	RMS	Relative error (%)	R	Slope	Intercept
$nL_w(443)/nL_w(555)$					
S03	0.168	19.05	0.70	*1.03*	*0.021*
R00	0.177	*18.42*	0.71	1.17	−0.13
K09	*0.167*	21.48	*0.82*	0.90	−0.063
$nL_w(490)/nL_w(555)$					
S03	*0.120*	*9.42*	*0.84*	0.96	0.070
R00	0.127	9.47	0.82	*1.03*	*−0.024*
K09	0.220	18.52	0.81	1.15	0.008
$nL_w(510)/nL_w(555)$					
S03	*0.084*	*6.10*	*0.85*	*0.83*	*0.17*
R00	0.089	6.40	0.82	0.85	0.14
K09	0.088	6.83	0.84	0.83	0.18

The numbers in italic represent the best statistical results.

Table 5
Same as Table 3 for the retrieved values of the aerosol optical properties: $\tau(865)$ and $\alpha(510)$.

	RMS	Relative error (%)	R	Slope	Intercept
$\tau(865)$					
S03	*0.033*	33.00	0.86	0.58	0.02
R00	0.035	*32.96*	0.87	0.57	0.02
K09	0.041	52.25	*0.87*	*0.99*	*0.02*
$\alpha(510)$					
S03	*0.566*	54.15	0.39	*0.37*	*0.93*
R00	0.618	71.15	0.30	0.22	1.35
K09	0.584	59.25	0.30	0.23	0.92

The numbers in italic represent the best statistical results.

algorithm to turbid waters, (Stumpf et al., 2003 and its update version, Bailey et al., 2010) and Ruddick et al. (2000), and one atmospheric correction algorithm, Kuchinke et al. (2009a), with a distinctly different, multispectral optimization approach. Results obtained using *in situ* data from three coastal sites (AAOT in the northern Adriatic Sea, MVCO and COVE in the northern Atlantic Bight) of the AERONET-OC network indicate that the estimates obtained with the S03 algorithm shows better accuracies on the overall *in-situ* dataset than the estimates given by the K09 and R00 alternative algorithms. This latter appears the least accurate.

An analysis of the main hypotheses of each atmospheric correction algorithm was presented showing a significant role of the aerosol models for R00 through the ratio of the aerosol reflectances and a large impact of the bio-optical model for S03. For K09, it is difficult to discern which assumption constrains the retrieval due to the non-linear inversion method. The fact that the aerosol models are very simple in K09 may explain the rather low accuracy for the estimates of the aerosol optical properties.

Even if S03 shows the best retrievals, the accuracy of results does not meet the requirements and improvements are needed. The three algorithms have hypothesis that could be mixed to improve the retrieval of the $nL_w(\lambda)$. Recent studies showed that the ratio of the water-leaving radiances is not so constant in the NIR, when seawater is very turbid (Doron, 2007; Ruddick et al., 2006). So depending of the level of turbidity, the value of the ratio will be either fixed or variable and this will constrain the retrieval of the $nL_w(\lambda)$. Another idea would be to estimate and retrieve the spectral shape of the $nL_w(\lambda)$. For turbid waters, the $nL_w(\lambda)$ at 412 and 443 nm is very low and this knowledge should be taken into account in the inversion schemes. Finally, a classification of the water types will help to use the "most-correct" bio-optical coefficients and will help to better estimate the $nL_w(\lambda)$ (Lubac & Loisel, 2007).

Acknowledgments

We thank the GSFC NASA for providing the SeaWiFS L1 data and to the SeaDAS team for the help and explanations in the use of the software. This work is supported by the French Spatial Agency (CNES) through the TOSCA program. Kevin Ruddick is funded by the Belgian Science Policy Office STEREO program (BELCOLOUR-2 project). Also thanks go to A. Girard and other MVCO maintenance staff in Woods Hole Oceanographic Institute for their support of the AERONET-OC instrument in MVCO Tower and Brent Holben and Ken Rutledge for managing and maintaining the COVE site. Finally, we thank David Dessailly for the technical help to modify the SeaDAS code and for processing the data. We thank the two anonymous reviewers for the comments and suggestions.

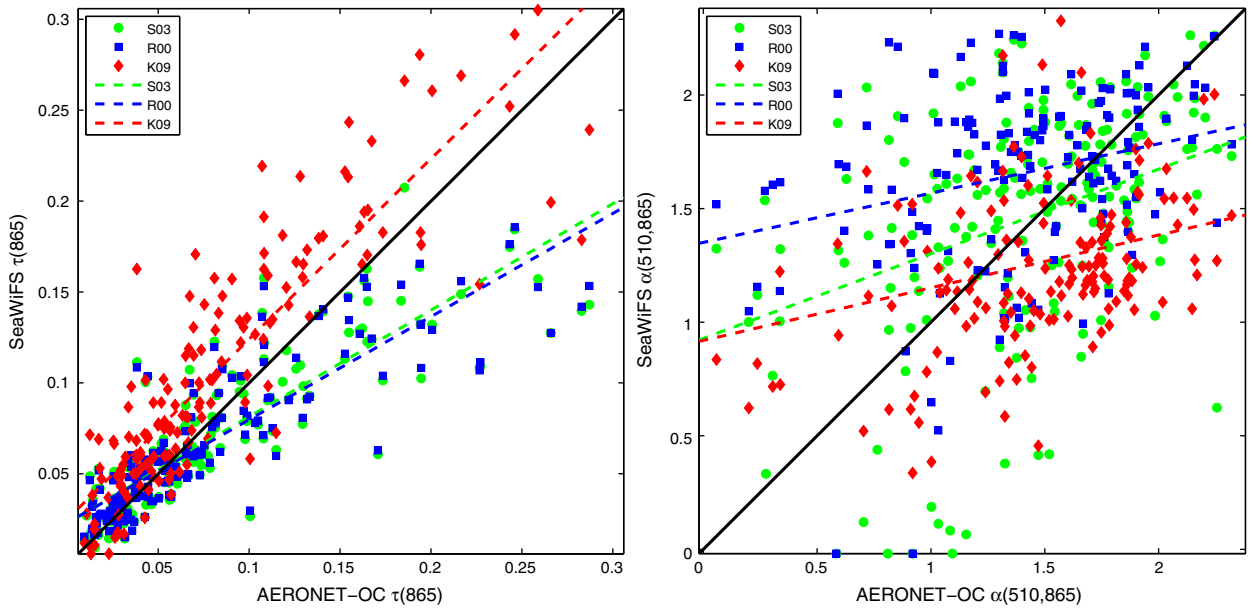

Fig. 4. Same as Fig. 1 but for the retrieved aerosol optical properties: $\tau(865)$ (left panel) and $\alpha(510)$ (right panel).

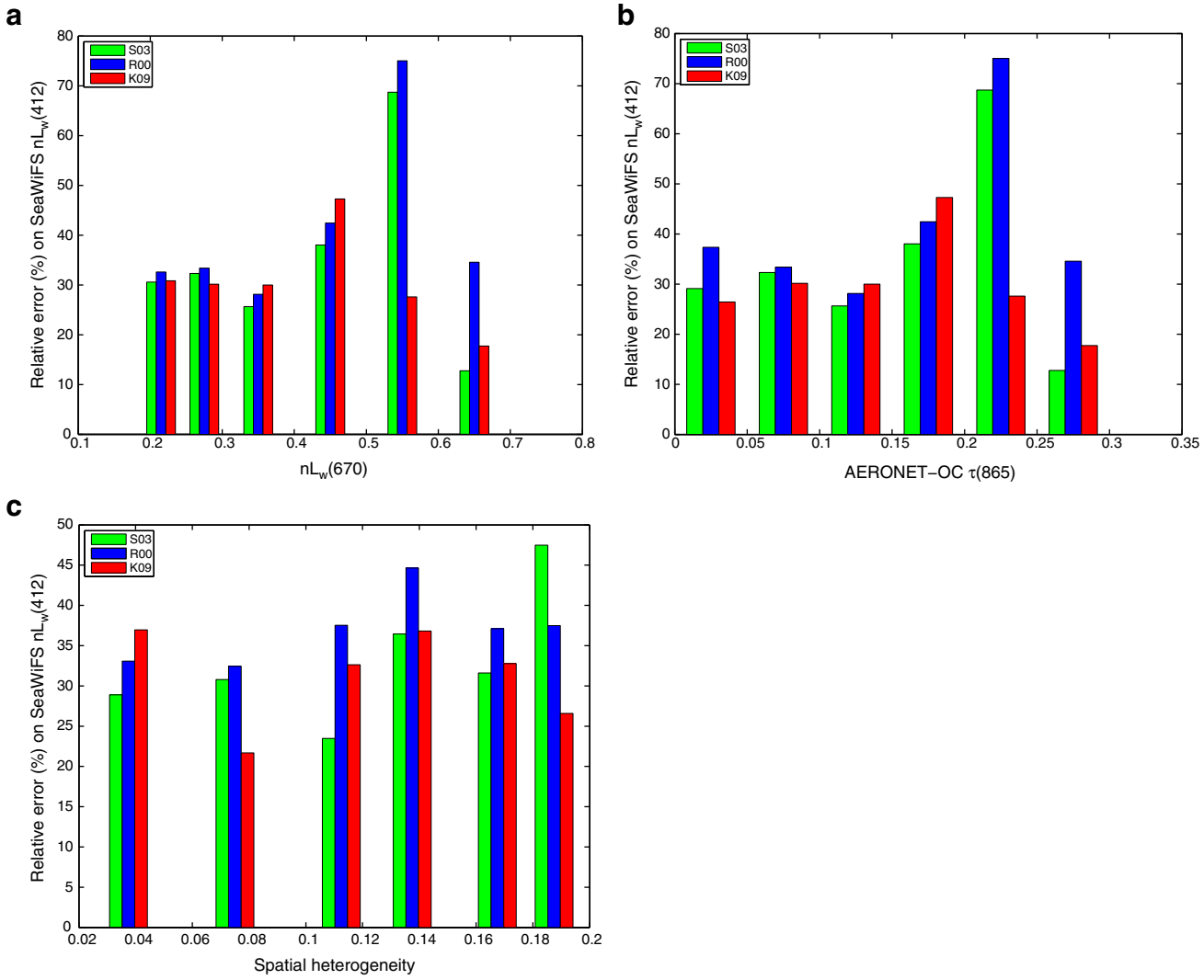

Fig. 5. Variation of the relative error on nLw(412) as a function of the values of (top to bottom): (i) $nL_w(670)$ (e.g., turbidity), (ii) $\tau(865)$ and (iii) the spatial homogeneity.

References

Ahmad, Z., Franz, B. A., McClain, C. R., Kwiatkowska, E. J., Werdell, J., Shettle, E. P., et al. (2010). New aerosol models for the retrieval of aerosol optical thickness and normalized water-leaving radiances from the SeaWiFS and MODIS sensors over coastal regions and open oceans. *Applied Optics*, *49*, 5545−5560.

Bailey, S., & Wang, M. (2001). Satellite aerosol optical thickness match-up procedures. *NASA technical memorandum, 2001-209982* (pp. 70−72). Greenbelt, MD: NASA Goddard Space Flight Center.

Bailey, S. W., Franz, B. A., & Werdell, P. J. (2010). Estimation of near-infrared water-leaving reflectance for satellite ocean color data processing. *Optics Express*, *18*, 7521−7527.

Baith, K., Lindsay, R., Fu, G., & McClain, C. R. (2001). SeaDAS, a data analysissystem for ocean-color satellite sensors. *Eos Transactions AGU*, *82*, 202.

Banzon, V. F., Gordon, H. R., Kuchinke, C. P., Antoine, D., Voss, K. J., & Evans, R. H. (2009). Validation of SeaWiFS dut-correction methodology in the Mediterranean Sea: Identification of an algorithm-switching criterion. *Remote Sensing of Environment*, *113*, 2689−2700.

Berthon, J. -F., & Zibordi, G. (2004). Bio-optical relationships for the northern Adriatic Sea. *International Journal of Remote Sensing*, *25*, 1527−1532.

Chomko, R. M., & Gordon, H. R. (1998). Atmospheric correction of ocean color imagery: Use of the Junge power-law aerosol size distribution with variable refractive index to handle aerosol absoprition. *Applied Optics*, *37*, 5560−5572.

Chomko, R. M., Gordon, H. R., Maritonera, S., & Siegel, D. A. (2003). Simultaneous retrieval of oceanic and atmospheric parameters for ocean color imagery by spectral optimization: A validation. *Remote Sensing of Environment*, *84*, 202−220.

Doron, M. (2007). Utilisation des données de couleur de l'océan pour estimer les propriétés optiques des eaux côtières: Caractérisation du signal marin dans le proche infrarouge pour les eaux turbides, développement d'algorithmes semi-analytiques, validation avec des données satellitaires, PhD dissertation, Université Pierre et Marie Curie, 183 pp.

Feldman, G. C., & McClain, C. R. (2009). In N. Kuring, & S. W. Bailey (Eds.), *Ocean color web, SeaWiFS reprocessing 2009.* : NASA Goddard Space Flight Centerhttp://www.oceancolor.gsfc.nasa.gov/.

Feng, H., Vandemark, D., Campbell, J. W., & Holben, B. N. (2008). Evaluation of MODIS ocean color products at a northeast United States coast site near the Martha's Vineyard Coastal Observatory. *International Journal of Remote Sensing*, *29*, 4479−4497.

Fu, G., Baith, K. S., & McClain, C. R. (1998). SeaDAS: The SeaWiFS data analysis system. *Proceedings of the 4th Pacific Ocean remote sensing conference, Qingdao, China, July 28–31* (pp. 73−79).

Garver, S., & Siegel, D. A. (1997). Inherent optical property inversion of ocean color spectra and its biogeochemical interpretation: 1 time series from the Sargasso Sea. *Journal of Geophysical Research*, *102*, 18607−18625.

Gordon, H. R. (1997). Atmospheric correction of ocean color imagery in the Earth Observing System era. *Journal of Geophysical Research*, *102*, 17081−17106.

Gordon, H. R., & Wang, M. (1994). Retrieval of water-leaving radiance and aerosol optical thickness over the oceans with SeaWiFS: A preliminary algorithm. *Applied Optics*, *33*, 443−452.

Gould, R. W., Arnone, R. A., & Sydor, M. (1998). Testing a new remote sensing reflectance algorithm to estimate absorption and scattering in case-2 waters. *SPIE Ocean Optics XII, Hawaï, USA*.

Hess, M., Koepke, P. L., & Schult, I. (1998). Optical properties of aerosols and clouds: The software package OPAC. *Bulletin of the American Meteorological Society*, *79*, 831−844.

Hooker, S. B., Esaias, W. E., Feldman, G. C., Gregg, W. W., & McClain, C. R. (1992). An overview of SeaWiFS and ocean color. In S. B. Hooker, & E. R. Firestone (Eds.), *NASA Tech Memo. 104566, Vol. 1*, Greenbelt, Maryland: NASA Goddard Space Flight Center 24 pp.

Hu, C., Carder, K. L., & Muller-Karger, F. E. (2000). Atmospheric correction of SeaWiFS imagery over turbid coastal waters. *Remote Sensing of Environment*, *74*, 195−206.

IOCCG (2000). Remote sensing of ocean colour in coastal, and other optically-complex, waters. In S. Sathyendranath (Ed.), *Reports of the International Ocean-Colour Coordinating Group, No. 3* (pp. 140). Darmouth, Canada: IOCCG.

IOCCG (2010). Atmospheric correction for remotely-sensed ocean-colour products. In M. H. Wang (Ed.), *Reports of the international ocean-colour coordinating group, no. 10* (pp. 78). Darmouth, Canada: IOCCG.

Kuchinke, C. P., Gordon, H. R., & Franz, B. A. (2009a). Spectral optimization for constituent retrieval in Case II waters I: Implementation and performance. *Remote Sensing of Environment*, *13*, 571−587.

Kuchinke, C. P., Gordon, H. R., Harding, L. W., Jr., & Voss, K. J. (2009b). Spectral optimization for constituent retrieval in Case II waters II: Validation study in the Chesapeake Bay. *Remote Sensing of Environment*, *113*, 610−621.

Land, P. E., & Haigh, J. D. (1996). Atmospheric correction over case 2 waters with an iterative fitting algorithm. *Applied Optics*, *35*, 5443−5451.

Lavender, S. J., Pinkerton, M. H., Moore, G. F., Aiken, J., & Blondeau-Patissier, D. (2005). Modification to the atmospheric correction of SeaWiFS ocean colour images over turbid waters. *Continental Shelf Research*, *25*, 539−555.

Loisel, H., & Morel, A. (1998). Light scattering and chlorophyll concentration in case 1 waters: A reexamination. *Limnology and Oceanography*, *43*, 847−858.

Lubac, B., & Loisel, H. (2007). Variability and classification of remote sensing reflectance spectra in the eastern English Channel and southern North Sea. *Remote Sensing of Environment*, *110*, 45−58.

Maritonera, S., Siegel, D. A., & Peterson, A. R. (2002). Optimization of semianalytical ocean color model for global scale applications. *Applied Optics*, *41*, 2705−2714.

Melin, F., Zibordi, G., & Berthon, J. -F. (2007). Assessment of satellite ocean color products at a coastal site. *Remote Sensing of Environment*, *110*, 192−215.

Morel, A., & Prieur, L. (1977). Analysis of variations in ocean color. *Limnology and Oceanography*, *22*, 709−722.

O'Reilly, J. E., Maritonera, S., Michell, B. G., Siegel, D. A., Carder, K. L., Garver, S. A., Kahru, M., & McClain, C. (1998). Ocean color chlorophyll algorithms for SeaWiFS. *Journal of Geophysical Research*, *103*, 24937−24953.

Oo, M., Vargas, M., Gilerson, A., Gross, B., Moshary, F., & Ahmed, S. (2008). Improving atmospheric correction for highly productive coastal waters using the short wave infrared retrieval algorithm with water-leaving reflectance constraints at 412 nm. *Applied Optics*, *47*, 3846−3859.

Ransibrahmanakul, V., Stumpf, R., Ramachandran, S., & Hughes, K. (2005). Evaluation of atmospheric correction algorithm for processing SeaWiFS data. *Proceeding SPIE*, *5885*, doi:10.1117/12.615722.

Robinson, W. D., Franz, B. A., Patt, F. S., Bailey, S. W., & Werdell, P. J. (2003). Masks and flags updates. In S. B. Hooker, & E. R. Firestone (Eds.), *SeaWiFS Postlaunch Technical Report Series, Chap.6, NASA/TM-2003-206892*, *Vol. 22*. (pp. 34−40).

Ruddick, K. G., De Cauwer, V., Park, Y. -J., & Mooe, G. (2006). Seaborne measurements of near infrared water-leaving reflectance: The similarity spectrum for turbid waters. *Limnology and Oceanography*, *51*, 1167−1179.

Ruddick, K. G., Ovidio, F., & Rijkeboer, M. (2000). Atmospheric correction of SeaWiFS imagery for turbid coastal and inland waters. *Applied Optics*, *39*, 897−912.

Shanmugam, P., & Ahn, Y. H. (2007). New atmospheric correction technique to retrieve the ocean colour from SeaWiFS imagery in complex coastal waters. *Journal of Optics A: Pure and Applied Optics*, *9*, 511−530.

Siegel, D. A., Wang, M., Maritonera, S., & Robinson, W. (2000). Atmospheric correction of satellite ocean color imagery: The black pixel assumption. *Applied Optics*, *39*, 3582−3591.

Stumpf, R. P., Arnone, R. A., Gould, R. W., & Ransibrahmanakul, V. (2003). A partly coupled ocean–atmosphere model for retrieval of water-leaving radiance from SeaWiFS in coastal waters. *NASA technical memorandum 2003-206892(22)* (pp. 51−59). Greenbelt, MD: NASA Goddard Space Flight Center.

Zibordi, G., Holben, B., Hooker, S. B., Melin, F., Berthon, J. -F., Slutsker, I., Giles, D., Vandemark, D., Feng, D., Rutledge, K., Schuster, G., & Al Mandoos, A. (2006). A network for standardized ocean color validation measurements. *EOS Transactions*, *87*, 293−297.

Zibordi, G., Holben, B., Slutsker, I., Giles, D., D'Alimonte, D., Mélin, F., Berthon, J. -F., Vandemark, D., Feng, H., Schuster, G., Fabbri, B. E., Kaitala, S., & Seppälä, J. (2009). AERONET-OC: A network for the validation of ocean color primary products. *Journal of Atmospheric and Oceanic Technology*, *26*, 1634−1651.

Zibordi, G., Melin, F., & Berthon, J. -F. (2006). Comparison of SeaWiFS, MODIS and MERIS radiometric products at a coastal site. *Geophysical Research Letters*, *33*, L06617, doi:10/1029/2006GL025778.